Neurochemical Research (2020) 45:1825–1838
https://doi.org/10.1007/s11064-020-03046-7

ORIGINAL PAPER

The Reducible Disulfide Proteome of Synaptosomes Supports a Role for Reversible Oxidations of Protein Thiols in the Maintenance of Neuronal Redox Homeostasis

Timothy D. Foley[1] · Giancarlo Montovano[1] · Monserrath Camacho Ayala[1]

Received: 5 March 2020 / Revised: 13 April 2020 / Accepted: 4 May 2020 / Published online: 12 May 2020

Abstract

The mechanisms by which neurons maintain redox homeostasis, disruption of which is linked to disease, are not well known. Hydrogen peroxide, a major cellular oxidant and neuromodulator, can promote reversible oxidations of protein thiols but the scope, targets, and significance of such oxidations occurring in neurons, especially in vivo, are uncertain. Using redox phenylarsine oxide (PAO)-affinity chromatography, which exploits the high-affinity of trivalent arsenicals for protein dithiols, this study investigated the occurrence of reducible and, therefore, potentially regulatory, protein disulfide bonds in Triton X-100-soluble protein fractions from isolated nerve-endings (synaptosomes) prepared from rat brains. Postmortem oxidations of protein thiols were limited by rapidly freezing the brains following euthanasia and, later, homogenizing them in the presence of the N-ethylmaleimide to trap reduced thiols. The reducible disulfide proteome comprised 5.4% of the total synaptosomal protein applied to the immobilized PAO columns and was overrepresented by pathways underlying ATP synaptic supply and demand including synaptic vesicle trafficking. The alpha subunits of plasma membrane Na^+, K^+-ATPase and the mitochondrial ATP synthase were particularly abundant proteins of the disulfide proteome and were enriched in this fraction by 3.5- and 6.7-fold, respectively. An adaptation of the commonly used "biotin-switch" method provided additional support for selective oxidation of thiols on the alpha subunit of the ATP synthase. We propose that reversible oxidations of protein thiols may underlie a coordinated metabolic response to hydrogen peroxide, serving to both control redox signaling and protect neurons from oxidant stress.

Keywords ATP synthase · Calcineurin · Disulfide proteome · Hydrogen peroxide · Mitochondria · Na+, K^+-ATPase · Oxidative stress · Phenylarsine oxide · Protein thiols · Redox signaling · Synaptosomes

Abbreviations

Biotin-HPDP	N-[6-(Biotinamido) hexyl]-3′-(2′-pyridyldithio)-propionamide
CaN	Calcineurin
DTT	Dithiothreitol
FT	Flow-through
GAPDH	Glyceraldehyde-3-phosphate dehydrogenase
GSH	Glutathione
KHH	Krebs–Henseleit–HEPES
LW	Last wash
LC–MS/MS	Liquid chromatography-tandem mass spectrometry
NEM	N-ethylmaleimide
NNT	Nicotinamide nucleotide transhydrogenase
PAO	Phenylarsine oxide
PPP	Pentose phosphate pathway
ROS	Reactive oxygen species
TCEP	Tris(2-carboxyethyl)phosphine
Trx	Thioredoxin

Electronic supplementary material The online version of this article (https://doi.org/10.1007/s11064-020-03046-7) contains supplementary material, which is available to authorized users.

✉ Timothy D. Foley
foleyt2@scranton.edu

[1] Department of Chemistry, University of Scranton, Scranton, PA 18510, USA

Introduction

Superoxide and hydrogen peroxide can be generated in neurons at multiple sites and are putative neuromodulators [1]. High output of these so-called reactive oxygen species

(ROS) by neuronal mitochondria, which appears to occur following strong Ca^{2+} influx [2] and during periods of inactivity [3], can also induce oxidative stress, a long-hypothesized cause of Alzheimer's disease and other aging-related neurodegenerative disorders [4]. Importantly, synaptic activity can promote transcriptional upregulation of antioxidant systems able to offset oxidant stress [5, 6]. However, post-translational mechanisms by which neurons can more rapidly adapt to elevated ROS and can coordinate necessary metabolic reprogramming with synaptic ATP demands are not well defined.

Hydrogen peroxide can, in principle, modulate diverse cellular processes by promoting reversible oxidations of regulatory and catalytic thiols on potentially numerous proteins by still unfolding pathways [7]. Protein thiol oxidation-based signaling activities of hydrogen peroxide, mediated in part by inactivation of protein phosphatases [7], must be balanced with protection against hydrogen peroxide-mediated oxidative stress. Thus, hydrogen peroxide can trigger the diversion of glucose from glycolysis to the NADPH-generating pentose phosphate pathway (PPP) [8] by oxidizing the essential catalytic thiol on glyceralde-3-phosphate dehydrogenase (GAPDH) [9]. The resulting increased rates of NADPH production support hydrogen peroxide removal, maintenance of reduced protein sulfur, and DNA repair by the thioredoxin (Trx) and glutathione (GSH) reducing systems [10]. A comprehensive understanding of the mechanisms by which hydrogen peroxide can signal metabolic adaptation in the cellular and subcellular compartments of all tissues, including the brain, will require that the targets of reversible oxidations of protein thiols, especially those operating in vivo, be established.

The scope of reversible oxidations of protein thiols occurring in the brain and other organs is uncertain for two reasons. First, protein thiol oxidation-based signaling paradigms have been informed mostly by studies of cultured cells exposed to generally high concentrations of hydrogen peroxide, conditions which likely allow bypass of kinetic restrictions to thiol oxidations operating in tissues [11]. The nature of reversible oxidations of protein thiols occurring in vivo has not been adequately investigated. Second, oxidations of protein thiols by hydrogen peroxide can give rise to sulfenic acids, mixed disulfides with glutathione (*S*-glutathionylation), and generally more stable protein disulfides [7]. Yet, even though potentially regulatory disulfide bonds can be distinguished from structural disulfide bonds in proteins by greater solvent exposure and propensity for reduction [12], redox signaling studies have focused more so on protein sulfenylation [13] and protein S-glutathionylation [14, 15]. The lack of a chemoselective method to capture, from tissues or cells, proteins forming reducible disulfide bonds has hindered an understanding of the significance of regulatory protein disulfide formation on a proteome-wide scale. This omission may be crucial as protein sulfenic acids and protein S-glutathionylated adducts can convert readily to protein disulfides following attacks by nearby thiols [16, 17]. Moreover, protein disulfides can form independently of these modifications following nitric oxide-induced *S*-nitrosylation [18] and by hydrogen peroxide-initiated redox relays involving abundant Trx peroxidases (peroxiredoxins) [19].

To address the need to study redox-sensitive protein disulfides on a proteome-wide scale with relevance to in vivo tissue redox states, we previously modified phenylarsine oxide (PAO)-affinity chromatography to enable capture of proteins containing reducible disulfide bonds [20] (Fig. 1). Like other trivalent arsenicals, PAO binds with high affinity to pairs of protein thiols that are vicinal (closely-spaced) by virtue of primary, tertiary, or quaternary structures, giving rise to dithioarsine rings [21]. The redox PAO-affinity method involves alkylation of reduced thiols followed by on-column reduction of protein disulfides with tris(2-carboxyethyl)phosphine (TCEP), making available PAO-binding vicinal thiols only on the proteins that contained reducible disulfide bonds. Rapid freezing of tissues immediately following animal euthanasia, combined with a thiol alkylation step during tissue homogenization, inhibit postmortem oxidations of protein and low-molecular-weight thiols [20, 22]. Using this approach, we previously concluded that about 5% of total proteins from homogenates of rat brains, representing functionally-diverse classes of intracellular proteins, contained reducible disulfide bonds [22].

The objective of the present study was to identify neuronal proteins targeted by reversible oxidations of thiols occurring in vivo. To this end, we used isolated nerve-endings (synaptosomes) prepared from N-ethylmaleimide (NEM)-alkylated homogenates from rat brains. Whole brains, rather than particular brain regions, were used as a source of synaptosomes to (i) eliminate the need for dissection, permitting rapid freezing of tissues, and (ii) limit the numbers of animals required to achieve sufficient synaptosomal protein. The findings establish the reducible disulfide proteome of synaptosomes and suggest that reversible oxidations of thiols on synaptic proteins may orchestrate a metabolic reprogramming necessary to terminate redox signaling and protect neurons from oxidative stress. In addition, results from both the PAO-affinity method and an adaptation of a commonly used "biotin-switch" technique [23], outlined in Fig. 1, highlight the alpha subunit of mitochondrial ATP synthase as a selective target of reversible protein thiol oxidations in neurons.

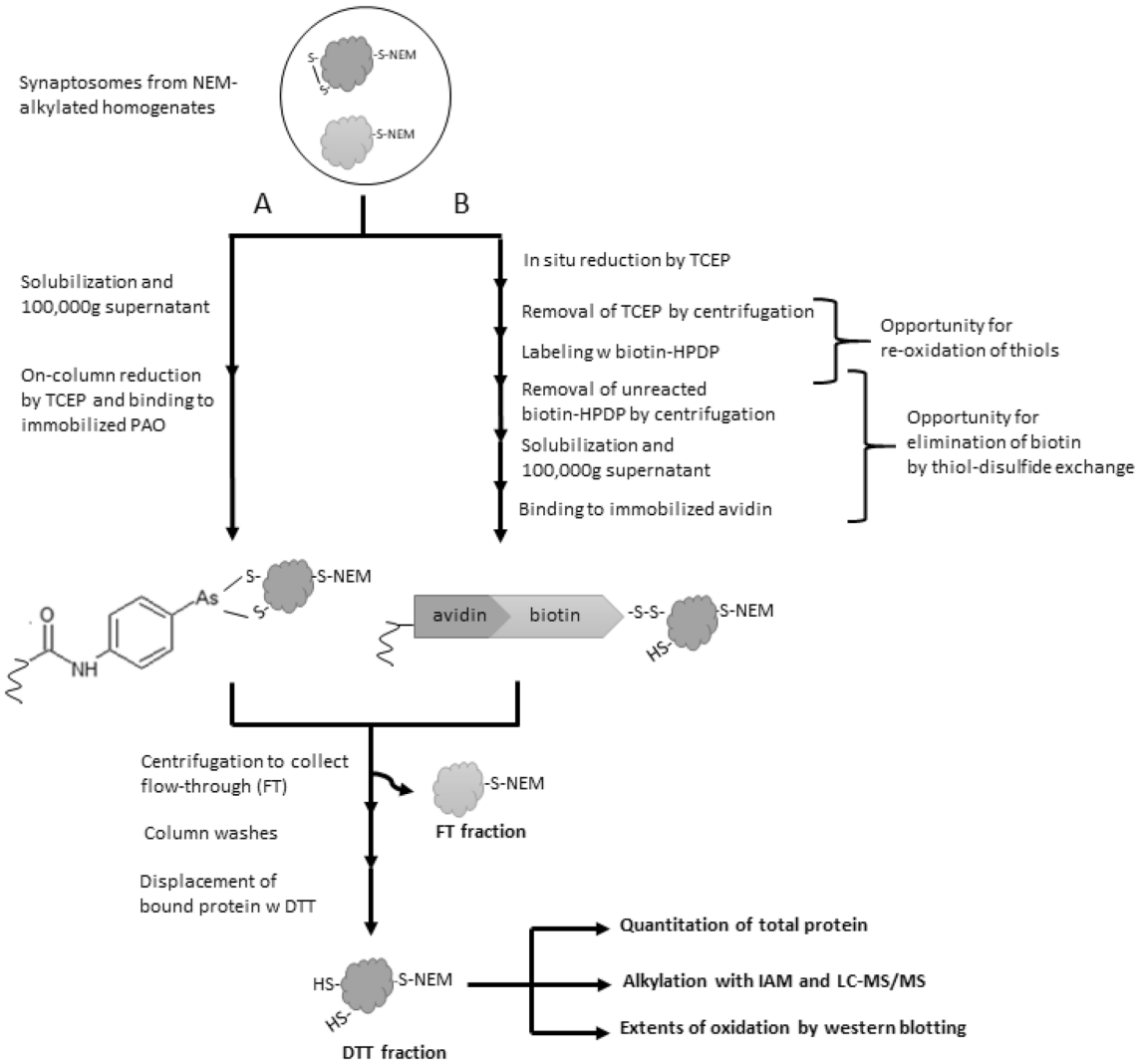

Fig. 1 Capture, from synaptosomes, of proteins containing reducible disulfide bonds and, more generally, reversibly oxidized thiols by **a** redox PAO-affinity chromatography and **b** an adaptation of the biotin-switch method combined with avidin-affinity chromatography. The PAO-affinity method offers the advantages of fewer steps and of not having to remove the reducing agent following reduction of disulfide bonds whereas opportunities exist for the re-oxidation of thiols and for the elimination of the biotin tag during the biotin switch procedure. On the other hand, the PAO-affinity technique should be chemoselective for disulfide bonds while the biotin switch approach is more likely to capture proteins containing regionally isolated thiols that have been stably modified to S-glutathionylated or S-nitrosylated adducts [23]

Materials and Methods

Materials

Protease Inhibitor Mini-Tablets, Coomassie Protein Assay, Imperial™ Protein Stain, TCEP, DTT, immobilized avidin, and EZ-Link N-[6-(Biotinamido)hexyl]-3′-(2′-pyridyldithio)propionamide (biotin-HPDP) were from Thermo-Fisher (Waltham, MA). Protean® TGX™ precast protein gels, nitrocellulose blotting membranes, Affi-Gel 10, and Mini Bio-Spin columns were from Bio-Rad (Hercules, CA). All antibodies were from Santa Cruz Biotechnology (Santa Cruz, CA). The specific primary antibodies used, and the dilutions applied, were as follows: alpha subunit of the Na^+, K^+-ATPase (sc-48345; 1:1000 dilution), the alpha subunit of mitochondrial ATP synthase (sc-136178; 1:1000 dilution), and calcineurin (sc-17808; 1:375). Horseradish peroxidase-linked mouse-IgG kappa binding protein (sc-516102) was used instead of a traditional secondary antibody. WesternSure® Premium chemiluminescent blotting substrate was from Li-Cor Biosciences (Lincoln, NE). All other reagents were from Millipore-Sigma (Burlington, MA).

Preparation of Synaptosomes

Brains were obtained from 5- to 6-week old male Sprague–Dawley rats following acclimation in our animal facility for two weeks. Whole brains were rapidly removed, snap-frozen in liquid nitrogen, and transferred to a -89 °C freezer for longer-term storage. On the day of use, four brains were partially thawed and homogenized at 10 mL/g of tissue in ice-cold homogenization buffer (0.32 M sucrose, 0.5 mM $MgSO_4$, 0.1 mM EGTA, 10 mM Tris, pH 7.4) containing 0.1 mM benzamidine·HCl, one Protease Inhibitor Mini-Tablet per brain, and 100 mM NEM. Homogenization was performed in a glass tube using 10 strokes with a Teflon pestle at 1250 rpm over 30 s. Homogenates were transferred to screw-cap vials and rotated for 60 min at room temperature (21–23 °C) to allow thiol alkylation. Following the alkylation period, synaptosomes were prepared by differential and Ficoll density gradient centrifugation at 4 °C as described by Michaelis et al. [24]. Experiments performed using batches of synaptosomes, prepared from four rat brains each and on different days, were considered biological replicates.

Preparation of Soluble and NEM-Free Synaptosomal Protein Fractions

Synaptosomes were resuspended with 3 mL of chromatography buffer (200 mM Tris, 0.2 mM benzamidine HCl, pH 7.4) containing 1% Triton X-100, 1 dissolved Protease Inhibitor Mini Tablet, and 100 mM NEM and allowed to incubate at room temp, while rotating, for 30 min. NEM was included to permit alkylation of any reduced protein thiols that may have become accessible as a result of the solubilization procedure. The resulting synaptosomal lysates were centrifuged at 100,000×*g* for 60 min to yield a supernatant containing both soluble and Triton X-100-solubilized proteins. Unreacted NEM was removed from the supernatants by centrifugal gel filtration as described by us previously [20, 22]. The protein concentrations of the supernatants were determined by the Coomassie Blue Assay using bovine serum albumin as standard.

Redox PAO-Affinity Chromatography

Redox PAO-affinity chromatography was performed as described by us previously [22] with minor modifications. Briefly, NEM-free synaptosomal proteins (0.6 mL containing 0.6–0.8 mg protein) were combined with 0.2 mL of packed immobilized PAO gel in Mini Spin columns and incubated for 1 h at room temperature (21–23 °C) both in the absence (control) and presence of TCEP (5 mM final). Subsequently, PAO columns were centrifuged briefly to collect unbound protein in the flow-through (FT) fractions. Following six washes, proteins bound to PAO were collected by centrifugation following resuspension of the PAO gels with 0.6 mL of chromatography buffer containing 100 mM DTT. Aliquots of Pre-column, FT, last wash (LW), and DTT fractions were diluted 1:1 with 80% glycerol, mixed, and stored at − 20 °C.

Biotin-Switch Method

Synaptosomes, prepared from NEM-alkylated homogenates as described above, were resuspended with 3 mL of Krebs–Henseleit-HEPES (KHH) buffer and incubated for 20 min at room temp in the absence and presence of TCEP (20 mM final) while rotating. Following the incubation period, synaptosomes were sedimented by centrifugation at 4 °C at 20,800 g for 10 min. TCEP was removed from the synaptosomes by resuspension in fresh KHH buffer and re-centrifugation. The membrane-permeable EZ-Link Biotin-HPDP was added from a 4 mM stock in dimethylformamide to achieve a final concentration of 0.04 mM and samples were incubated for an additional 20 min at room temp while rotating. Unreacted biotin-HPDP was removed following sedimentation of the synaptosomes for 10 min at 20,800 g. Synaptosomes were washed once by resuspension with KHH buffer and re-centrifugation.

Immobilized Avidin-Affinity Chromatography

Synaptosomes were solubilized by adding 5 volumes of lysis buffer (3 mM Tris, 10 uM benzamidine HCl, pH 8.5) containing 1% (v/v) Triton X-100 and placement on ice for 30 min with brief vortex mixing every 5 min. Following centrifugation for 1 h at 100,000×*g*, supernatants containing solubilized proteins (0.6 mL containing 0.6–0.8 mg protein) were combined with 0.1 mL packed avidin agarose gels in Mini-Spin columns and allowed to incubate for 1 h at room temp. Unbound (flow-through; FT) protein was collected by brief centrifugation. Following repeated (6x) washes to remove weakly bound proteins, the immobilized avidin columns were resuspended with 0.1 mL of buffer containing 50 mM DTT to cleave the disulfide bonds linking the bound proteins to biotin. Pre-column fractions, together with the collected FT, last wash, and DTT fractions were diluted 1:1 with 80% (v/v) glycerol and stored at – 20 °C until analyses.

Analyses of PAO-Affinity and Avidin-Affinity Column Fractions

Column fractions (20 µL) were diluted 1:1 with reducing Laemmli sample buffer, heated for 5 min at 95 °C, and resolved by gel electrophoresis on 4–20% Mini-Protean® TGX™ precast protein gels (10-well, 50 µL) at 150 V. Following electrophoresis, proteins were either stained for

total protein with Imperial™ Protein Stain or transferred to 0.2 µM nitrocellulose blotting membranes. For blots probing the alpha subunit of Na^+, K^+-ATPase, protein samples were not heated prior to sample loading. The specific antibodies used, and the dilutions applied, are listed under Materials. Blots were developed using WesternSure® Premium chemiluminescent blotting substrate and the C-DiGit Blot Scanner (Li-Cor Biosciences) and analyzed using Image Studio™ software (Li-Cor Biosciences).

Representative DTT-eluted samples were run onto gels briefly but not resolved. Unresolved gel bands were excised and shipped to MSBioworks LLC (Ann Arbor, MI) for alkylation of reduced thiols with iodoacetamide, in-gel tryptic digestion, and protein identification by LC–MS/MS using a Waters NanoAcquity HPLC system interfaced to a ThermoFisher Q Exactive. Data were searched using Mascot and filtered using a 1% protein and peptide FDR and requiring at least two unique peptides per protein. Proteins reported are those identified by MSBioworks in two out of two analyses. Protein cysteine residues labeled by iodoacetamide, giving rise to carbamidomethyl groups, were assumed to be sites of reversible oxidations.

Pathway Overrepresentation Analysis

A statistical overrepresentation test was run through the Gene Ontology Resource (https://geneontology.org/) using the Protein Analysis Through Evolutionary Relationships (PANTHER) classification system [25] using the rat protein database. The accession numbers of all 125 proteins identified in the synaptosomal disulfide proteome were included. Nonredundant pathways are reported for which enrichment was at least 25-fold and to which at least four sample proteins were assigned. The number of proteins from the organism (rat) assigned to each pathway, the number of proteins from the sample (disulfide proteome) assigned to each pathway, the fold-enrichment of each pathway in the sample, and the false discovery rate, a measure of confidence in proteomics datasets, are reported.

Results

A Fraction of Synaptosomal Proteins Contains Reducible Disulfide Bonds

Alkylated and detergent-solubilized synaptosomal proteins were fractionated by PAO-affinity chromatography (Fig. 1) to yield proteins, in the DTT-eluted fractions, containing PAO-binding thiols that had been oxidized to disulfide bonds prior to the concomitant alkylation and homogenization step. Figure 2a shows a representative Coomassie blue-stained gel of synaptosomal protein fractions generated by the redox PAO-affinity procedure. Importantly, almost no protein was detectable in DTT-eluted fractions after incubations of samples with immobilized PAO in the absence of TCEP indicating that most PAO-binding thiols were (i) alkylated by the NEM or (ii) oxidized and, in either case, unable to bind PAO in a DTT-sensitive manner. Inclusion of TCEP during the incubations of synaptosomal protein with the immobilized PAO, however, increased the amount of protein eluting in the DTT fractions (Fig. 2a). The population of proteins that bound to the PAO in a TCEP-dependent and DTT-sensitive manner was considered to have contained vicinal thiols reversibly oxidized to presumed disulfide bonds.

The results of the redox PAO-affinity fractionation were highly reproducible, both quantitatively and qualitatively, across three biological replicates, each performed using synaptosomes prepared from four rat brains. The percentage of total synaptosomal protein, by mass, containing reversibly oxidized thiols was determined to be 5.4% (SD = 0.3%). In addition, the protein composition of the DTT-eluted fractions from all three batches of synaptosomes was indistinguishable following gel electrophoretic resolution, showing especially prominent bands at approximately 60 kDa and 45 kDa (Fig. 2a).

Mitochondrial Metabolic Pathways are Highly Overrepresented by Proteins of the Synaptosomal Disulfide Proteome

LC–MS/MS analyses of proteins from a representative DTT fraction identified 125 proteins detected in both of two replicate determinations (Supplementary Table S1). In addition, differential thiol labeling by NEM (added prior to reduction of disulfides) and iodoacetamide (added after reduction of disulfides) identified 67 cysteine residues on 30 proteins that were carbamidomethylated by the iodoacetamide, suggesting these cysteines were sites of reversible oxidations (Supplementary Table S1). The seemingly most abundant proteins, ranked by total mass spectral counts, were catalytic (alpha) subunit isoforms of Na^+, K^+-ATPase, the alpha subunit of mitochondrial ATP synthase, actin, the 75 kDa subunit of mitochondrial complex I, and mitochondrial aconitate hydratase (Table 1, Supplementary Table S1). Spectral counts, the number of spectra identified for a protein, are a generally accepted, cost-effective, and semi-quantitative index of relative protein abundance in label-free proteomic samples although caution should be applied as the ionization efficiencies of peptides can vary [26]. It is noteworthy that the molecular weights of the alpha subunit of the ATP synthase (59.8 kDa) and actin (41.7 kDa) are near the relative molecular weights of the prominent gel bands at 60 kDa and 45 kDa (Fig. 2a). Among protein kinases and phosphatases, the highest-ranking protein was the catalytic subunit of the serine/threonine protein phosphatase calcineurin (CaN)

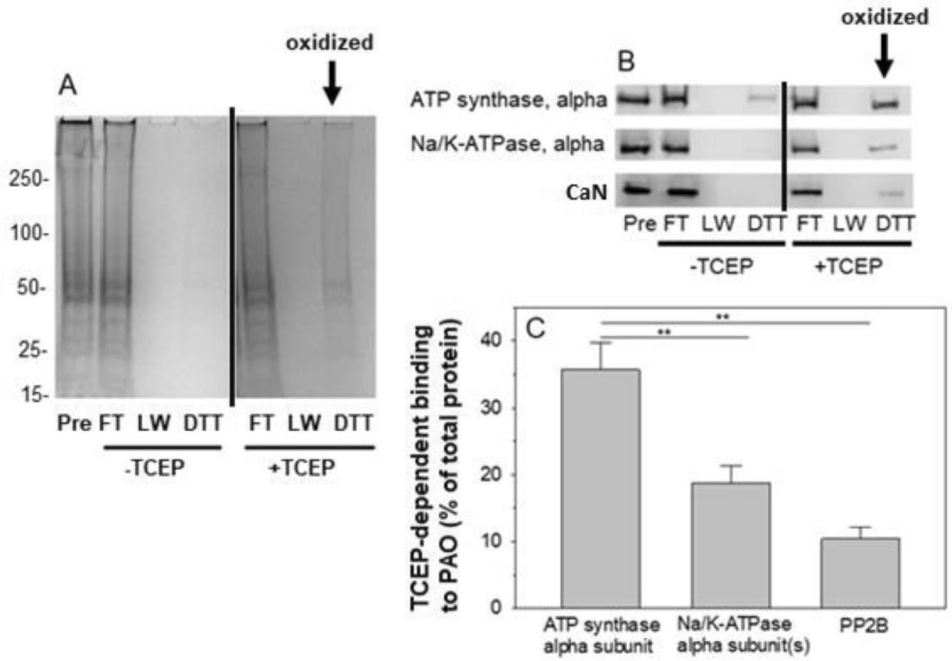

Fig. 2 Redox PAO-affinity chromatography demonstrates that a fraction of synaptosomal protein contains reversibly oxidized thiols. Triton X-100-soluble synaptosomal extracts prepared from NEM-alkylated brain homogenates were subjected to gel filtration, to remove unreacted NEM, and fractionation by redox PAO-affinity chromatography in the absence and presence of TCEP (5 mM final). **a** Total protein gel visualized with Imperial™ Protein Stain (ThermoFisher) showing positions of molecular weight markers. Samples were generated from fractionation of a representative synaptosome preparation obtained from four rat brains. Nearly identical results were obtained for three biological replicates. **b** Chemiluminescent western blots for the indicated proteins obtained using a C-DiGit Blot Scanner (Li-COR). **c** The percentage of each protein of interest binding the immobilized PAO in a TCEP-dependent and DTT-sensitive manner calculated from western blot band intensities obtained using Image Studio software version 5.2. Values represent the mean ± SD for technical replicates (n = 4–5) using samples generated from fractionation of a representative synaptosome preparation. Vertical black lines indicate lane splicing on gels and blots. *Pre* pre-column, *FT* flow-through, *LW* last wash. **P < 0.01 by unpaired t-test comparisons to the ATP synthase alpha subunit

Table 1 The most abundant proteins of the synaptosomal disulfide proteome

Rank	Identified proteins	Gene	Accession number	SpC	% Cov	Cys(ox)
1	Sodium/potassium-transporting ATPase alpha subunits	Atp1a3	P06687	127	50	C695
		Atp1a2	P06686	117	47	C702
		Atp1a1	P06685	101	41	C705
2	ATP synthase subunit alpha, mitochondrial	Atp5f1a	P15999	85	52	ND
3	Actin, cytoplasmic 1	Actb	P60711	65	51	ND
4	NADH-ubiquinone oxidoreductase 75 kDa subunit, mitochondrial	Ndufs1	Q66HF1	58	52	C64; C78; C176; C179
5	Aconitate hydratase, mitochondrial	Aco2	Q9ER34	52	41	C384

The top proteins identified in the DTT-eluted fractions in both of 2 replicate LC–MS/MS analyses are listed, ranked by total mass spectral counts (SpC). The complete list can be found in Supplementary Table S1. Differential thiol labeling by NEM (prior to disulfide reduction) and by iodoacetamide (following disulfide reduction) identified carbamidomethylated cysteine residues which represent likely sites of reversible oxidations [Cys(ox)]. ND, not detected among the peptides identified and sequenced. %Cov, percent coverage of the complete amino acid sequence

(Supplementary Table S1), an enzyme enriched in presynaptic terminals [27].

Panther Pathway overrepresentation analysis highlighted four pathways that were enriched among this population of proteins by at least 25-fold: the tricarboxylic acid (TCA) cycle, ATP synthesis, synaptic vesicle trafficking, and glycolysis (Table 2).

Table 2 Pathways overrepresented by the synaptosomal disulfide proteome

Rank	Pathway	# Proteins organism	# Proteins Sample	Fold-Enrichment	FDR
1	TCA cycle	11	5	81.3	8.33×10^{-7}
2	ATP synthesis	11	4	65.1	3.23×10^{-5}
3	Synaptic vesicle trafficking	28	7	44.7	6.67×10^{-8}
4	Glycolysis	50	7	25.0	9.48×10^{-7}

FDR false discovery rate

A statistical overrepresentation test was run through the Gene Ontology Resource using the PANTHER Classification System [25]. Pathways listed are those that were enriched by at least 25-fold and to which at least four sample proteins were assigned

The Catalytic Alpha Subunits of the Plasma Membrane Na^+, K^+-ATPase and the Mitochondrial ATP Synthase are Enriched in the Synaptosomal Disulfide Proteome.

The relative immunoreactive band intensities, in the fractions generated by PAO-affinity chromatography, of the top two protein hits, namely the alpha subunits of Na^+, K^+-ATPase and ATP synthase, were determined by western blotting (Fig. 2b, c). The band intensities of CaN, as a key regulator of Na^+, K^+-ATPase [28] and synaptic vesicle endocytosis [29], were also examined. The Na^+, K^+-ATPase antibody used recognizes all three alpha isoforms. Importantly, neither the Na^+, K^+-ATPase alpha subunit nor CaN was detected in DTT fractions obtained from protein samples incubated with immobilized PAO in the *absence* of TCEP while only a small amount of the ATP synthase alpha subunit could be detected in these fractions. Similar to the results for total protein (Fig. 2a), inclusion of TCEP increased the amounts of each of these proteins detected in the DTT fraction (Fig. 2b).

The TCEP-dependent band intensities of each protein in the DTT fractions (representing oxidized protein) were determined by densitometry and divided by the band intensities of each protein in the Pre column fractions (representing total protein) to estimate the fractions of each protein containing reversibly oxidized PAO-binding thiols (Fig. 2c). These values were about 10% for CaN, 19% for the alpha subunit(s) of Na^+, K^+-ATPase, and 36% for the alpha subunit of ATP synthase. Thus, all three of these proteins were enriched in the disulfide proteome compared to total synaptosomal protein which, as noted above, exhibited an average of only 5.4% oxidation. The 6.7-fold enrichment of the alpha subunit of ATP synthase was particularly noteworthy.

An Alternate Redox Method Provides Further Support for Selective Oxidations of Thiols on the Alpha Subunit of Mitochondrial ATP Synthase in Synapses

In a related experiment, the reversibly oxidized proteome of synaptosomes was investigated using an adaptation (Fig. 1) of the commonly employed biotin-switch approach [23]. Synaptosomes, prepared from NEM-alkylated brain homogenates, were incubated with and without (control) TCEP to reduce reversibly oxidized thiols. Following removal of TCEP by centrifugation, synaptosomes were resuspended in buffer containing the membrane-permeable biotin-HPDP. An additional "minus TCEP" control received no biotin-HPDP. Following removal of unreacted biotin-HPDP by centrifugation, detergent solubilization, and centrifugation at 100,000×*g*, the resulting supernatants were applied to immobilized avidin-affinity columns. Unbound protein was collected in the FT fraction. Following repeated washing, proteins containing formerly oxidized and now biotinylated thiols were removed by addition of DTT, which cleaves the disulfide bonds linking the proteins to avidin-bound biotin.

In each of two biological replicates, only about 1% of synaptosomal protein applied to the immobilized avidin eluted in the DTT fraction from samples treated with TCEP and biotin-HPDP (Fig. 3a), compared to 5.4% in the redox PAO-affinity experiment described above. Indeed, only 13 proteins were identified by LC–MS/MS in both of two technical replicate measures performed (Table 3), suggesting that many proteins in this sample may have been below the threshold for detection. Thus, the apparent yield of proteins containing reversibly oxidized thiols by the biotin-switch technique was substantially lower. As such, the DTT fractions (including the controls) obtained by the biotin-switch method were concentrated tenfold to visualize the proteins in these fractions on Coomassie blue-stained gels (Fig. 2a).

Protein was clearly visible in the 10x-concentrated DTT-eluted fractions from samples that had been treated both with TCEP to reduce reversibly oxidized thiols and with biotin-HPDP to label the newly reduced thiols. Notably, the electrophoretic banding pattern was qualitatively similar to that of the DTT fractions obtained by the PAO-affinity method, also showing relatively prominent bands at about 60 kDa and 45 kDa (Fig. 3A). Importantly, much less protein was observed in the DTT-eluted fractions from control samples that had not been treated with TCEP but were exposed to biotin-HPDP. Moreover, no protein was visible in DTT-eluted fractions generated from samples exposed neither to TCEP nor to biotin-HPDP.

Comparable to the DTT fractions obtained by the redox PAO-affinity method, the alpha subunit of the mitochondrial ATPase and actin also appeared to be relatively abundant

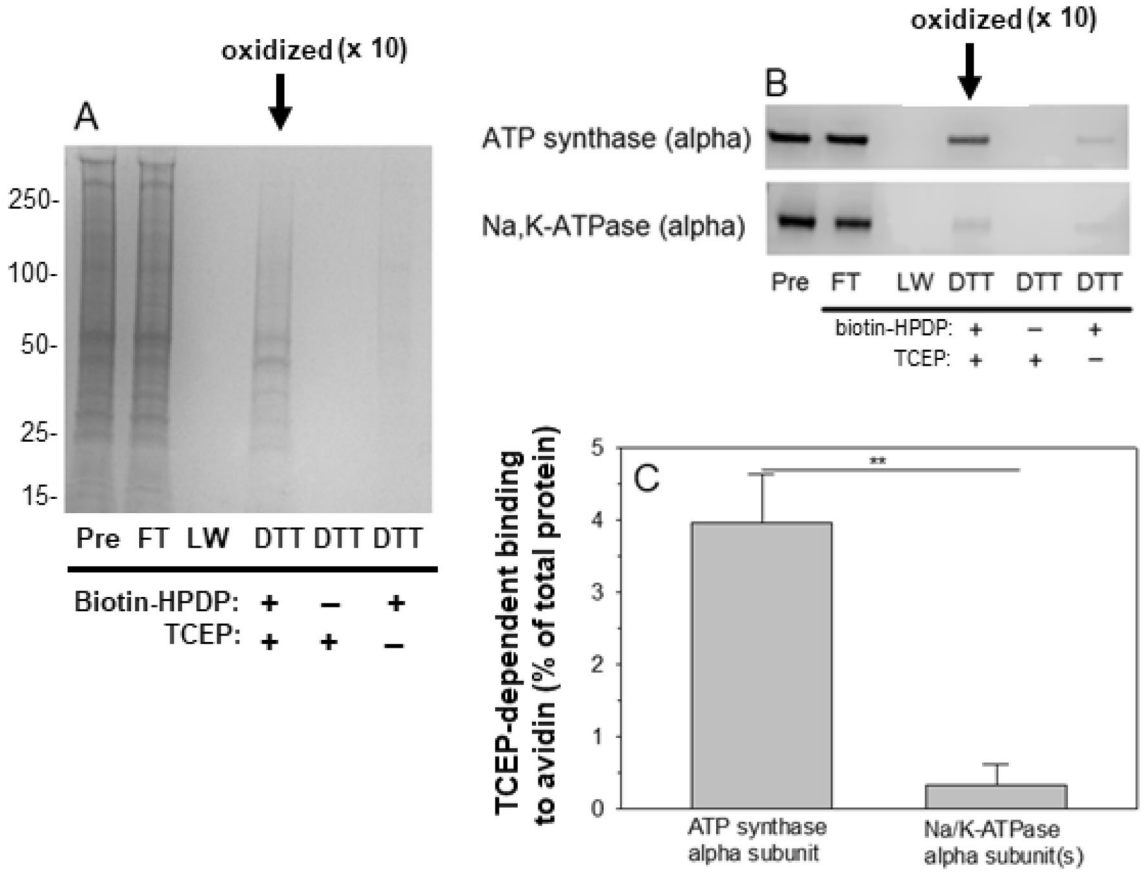

Fig. 3 The biotin-switch method provides further support for selective oxidations of thiols on the alpha subunit of mitochondrial ATP synthase. Following treatments with and without TCEP, synaptosomes prepared from NEM-alkylated brain homogenates were incubated in the absence and presence of biotin-HPDP. A second "minus TCEP" control received no biotin-HPDP. Subsequently, solubilized synaptosomal protein fractions were prepared and proteins containing formerly oxidized and now biotinylated thiols were allowed to bind immobilized avidin. Following collection of the flow-through (FT) fraction and extensive washing, bound proteins were removed by addition of DTT. All DTT-eluted fractions, including the controls, were collected in volumes of buffer that were one-tenth the volumes of samples applied to the avidin columns to achieve tenfold concentrations. **a** A total protein gel stained with Imperial™ Protein Stain (ThermoFisher) and showing positions of molecular weight markers. Samples were generated from fractionation of a synaptosome preparation obtained from four rat brains. Nearly identical results were obtained in two biological replicates. **b** Chemiluminescent western blots for the indicated proteins using a C-DiGit Blot scanner (LiCOR). **c** The percentage of each protein of interest binding the immobilized avidin in a TCEP-dependent and DTT-sensitive manner calculated from western blot band intensities obtained using Image Studio software version 5.2. Values represent the mean ± S.D. for technical replicates (n = 3) using samples generated from fractionation of a representative synaptosome preparation. *Pre* pre-column, *FT* flow-through, *LW* last wash. **P < 0.01 by unpaired t-test comparisons to the ATP synthase alpha subunit

in DTT fractions obtained by the biotin-switch procedure, based on total spectral counts (Table 3) and in agreement with the relatively prominent gel bands at about 60 kDa and 45 kDa (Fig. 3A). Other identified proteins included the alpha3 subunit of the Na^+, K^+-ATPase and the ADP/ATP translocase 1.

The relative intensities, in the avidin-affinity fractions, of the ATP synthase alpha subunit and, for comparison, the Na^+, K^+-ATPase alpha subunit were examined by western blotting using, as above (Fig. 2a), the antibody that recognizes all three Na^+, K^+-ATPase alpha isoforms (Fig. 3b). Similar to the total protein gel, the band intensities of the ATP synthase alpha subunit, although not the Na^+, K^+-ATPase alpha subunit, were much lower in DTT-eluted fractions from samples that were not treated with TCEP. Neither protein was detected in DTT fractions from samples exposed neither to TCEP nor to biotin-HPDP. The difference in band intensities of the −TCEP/DTT samples and the +TCEP/DTT samples were divided by the band intensities of the Pre column samples and subsequently divided by 10 (to correct for the tenfold concentration of the DTT samples) to estimate the fractions of each protein binding the immobilized avidin-affinity column in a TCEP-dependent and DTT-sensitive manner (Fig. 2C). The obtained values were 4.0% for the ATP synthase alpha subunit and 0.33% for the Na^+, K^+-ATPase alpha subunits. Therefore, the alpha subunit of

Table 3 Synaptosomal proteins containing reversibly oxidized thiols identified by the biotin-switch method

Rank	Identified proteins	Gene	Accession number	SpC	% Cov	Redox PAO-affinity
1	ATP synthase subunit alpha, mitochondrial	Atp5f1a	P15999	39	31	X
2	Actin, cytoplasmic 1	Actb	P60711	35	32	X
3	Sodium/potassium-transporting ATPase subunit alpha-3	Atp1a3	P06687	22	12	X
4	ADP/ATP translocase 1	Slc25a4	Q05962	9	17	X
5	Histone H4	Hist1h4b	P62804	8	31	X
6	Histone H2B type 1		Q00715	8	34	
7	Histone H3.3	H3f3b	P84245	8	21	
8	Malate dehydrogenase, mitochondrial	Mdh2	P04636	7	13	X
9	Myelin proteolipid protein	Plp1	P60203	7	12	X
10	Cytochrome b-c1 complex subunit 1, mitochondrial	Uqcrc1	Q68FY0	6	7	X
11	Citrate synthase, mitochondrial	Cs	Q8VHF5	6	9	X
12	Cytochrome c oxidase subunit 5A, mitochondrial	Cox5a	P11240	4	12	X
13	Aconitate hydratase, mitochondrial	Aco2	Q9ER34	4	4	X

Proteins identified in the DTT-eluted fractions in both of 2 replicate LC–MS/MS analyses are listed, ranked by total mass spectral counts (SpC). % Cov, percent coverage of the complete amino acid sequence. Proteins identified also by the redox PAO-affinity method are noted

the ATP synthase was enriched in the reversibly oxidized thiol proteome captured by the biotin-switch technique by about fourfold compared to total protein and by about 12-fold compared to the Na^+, K^+-ATPase alpha subunits.

Discussion

The results of this work establish the reducible disulfide proteome of synaptosomes under conditions designed to limit postmortem oxidations of thiols. The finding that about 5% of total synaptosomal protein contained reducible disulfide bonds argues that potentially regulatory protein thiol oxidations can occur in synapses, in vivo, and extends our previous observations using whole brain homogenates [22, 30]. The major novel findings of the present study are that the synaptosomal disulfide proteome was highly overrepresented by pathways, or enriched with specific proteins, mediating both the supply (TCA cycle, ATP synthesis, glycolysis) and demand (synaptic vesicle trafficking, Na^+, K^+-ATPase) for ATP in synapses. In particular, the catalytic alpha subunits of plasma membrane Na^+, K^+-ATPase isoforms and mitochondrial ATP synthase appeared to be the most abundant proteins of the disulfide proteome and were enriched in the oxidized protein fraction by 3.5-fold and 6.7-fold, respectively.

The molecular basis for TCEP-dependent binding to immobilized PAO can be rationalized for many of the proteins identified in the synaptosomal disulfide proteome. For example, specific cysteine residues contributing to closely spaced pairs or clusters of thiols were found to be oxidized, presumably to disulfide bonds, on several proteins. These included GAPDH (C150 and C154), enolase (C337, C339, C357, C389), dihydrolipoyl dehydrogenase (C80, C85), and cytochrome c oxidase subunit 5B (C113, C116). Other proteins of the synaptosomal disulfide proteome identified here, such as the alpha subunit of the Na^+, K^+-ATPase [31], actin [32], tubulin [33], and the ADP/ATP translocase [34], have been reported previously to form intramolecular disulfide bonds in response to oxidative stress.

A search of the Uniprot database [35] revealed that a small fraction (< 5%) of the 125 proteins identified in the synaptosomal disulfide proteome, namely contactin-1, albumin, the beta subunit of Na^+, K^+-ATPase, neural cell adhesion molecule 1, neuronal membrane glycoprotein, and myelin proteolipid protein, contain *structural* disulfide bonds. Furthermore, cysteine residues participating in the structural disulfides in these proteins were found here to be reversibly oxidized (Supplementary Table S1). These results argue strongly, although not surprisingly, that required experimental manipulations, for example, tissue homogenization, thiol alkylation, and/or detergent solubilization, induced protein unfolding sufficient to expose buried structural disulfide bonds in some proteins. Indeed, we have observed aggregation of proteins following prolonged alkylation at elevated temperatures and in the absence of detergent, suggesting that the alkylation step may be an especially important trigger of protein unfolding (Foley et al., unpublished observations). Importantly, however, because the occurrence and location of structural disulfide bonds in proteins is well established, these disulfides can be readily eliminated from consideration as possible redox-sensitive regulatory sites. Moreover, any experimentally-induced protein unfolding should increase neither the formation of regulatory disulfides, as

the alkylation step traps reduced thiols during tissue homogenization, nor the reducibility of regulatory disulfide bonds as these disulfides should already be solvent-exposed [12].

The present findings that a large fraction (36%) of the alpha subunit of mitochondrial ATP synthase contained reversibly oxidized thiols argue that this subunit may be preferentially oxidized to disulfide bonds in presynaptic compartments, in vivo. We identified this subunit previously in the disulfide proteome from brain homogenates [22] but did not examine the degree of oxidation. Among the targets of protein thiol oxidations in the healthy brain which we have analyzed so far for the extents of oxidation, including GAPDH [30], an established oxidant-sensitive protein [9], none of these have been as highly enriched in the oxidized protein fractions as the alpha subunit of the ATP synthase was here. In a single test of samples generated in the present study, 16% of GAPDH was found to contain reversibly oxidized thiols (Foley et al., unpublished observation), giving rise to an approximate threefold enrichment in the disulfide proteome, a value comparable to what we observed previously among proteins from brain homogenates [30]. Limited studies by other groups also support a high propensity for thiols on the alpha subunit of the ATP synthase to be reversibly oxidized. Specifically, experiments using isolated brain mitochondria revealed that thiols on the alpha subunit were selectively oxidized, by S-glutathionyation, following in vitro depletion of respiratory substrates or exposure of the mitochondria to low concentrations of hydrogen peroxide [36]. In addition, up to 65% of this subunit was found to contain reversibly oxidized thiols, attributed mostly to S-glutathionylation, in Xenopus laevis oocytes [37]. Experiments by both of these groups demonstrated that reversible oxidations of thiols on the alpha subunit were associated with profound inhibition of ATP synthase activity [36, 38].

The basis for the TCEP-dependent binding of the alpha subunit of ATP synthase to immobilized PAO reported here is uncertain and warrants consideration. This polypeptide contains only two cysteine residues and the thiol groups of these are far apart (14.8 angstroms) in the crystal structure [39]. We envision two possibilities, both of which might involve S-glutathionylation. First, large conformational changes can be triggered in proteins by oxidations of one thiol, for example by S-glutathionylation, which can bring distant pairs of thiols into disulfide bonding distance [40]. Second, TCEP-mediated reversals of oxidations occurring independently on both thiols, also for example by S-glutathionylation, followed by a PAO-induced protein conformational change might underlie the binding of the alpha subunit to PAO. Indeed, a substantial fraction of the alpha subunit was found to be S-glutathionylated at *both* cysteine residues in the study of Xenopus oocytes [37]. It is plausible that a similar explanation might underlie the TCEP-dependent binding to PAO of other proteins of the synaptosomal disulfide proteome. For instance, the alpha subunit of Na^+, K^+-ATPase can be S-glutathionylated at multiple cysteine [41] residues, including the conserved cysteine residue (C695 in alpha3) found by us to be reversibly oxidized in all three alpha isoforms (Supplementary Table S1). Importantly, S-glutathionylation of the Na^+, K^+-ATPase alpha subunit is also linked to inhibition of enzyme activity [41].

We propose that reversible oxidations of thiols on many of the synaptosomal proteins identified here may coordinate neuronal responses to hydrogen peroxide (Fig. 4), with implications for both the termination of redox signaling and the protection of neurons against oxidative stress. Oxidative inhibition of ATP synthase activity may play an especially important role in this regard as it should increase the energy available from the H^+ gradient across the inner mitochondrial membrane necessary to drive NADPH production by the nicotinamide nucleotide transhydrogenase (NNT) [42]. NNT is the major source of NADPH necessary to support the mitochondrial Trx and GSH systems [42, 43]. Oxidative inhibition of citric acid cycle and electron transport enzymes, also reported here to be targeted by thiol oxidations, should diminish mitochondrial ROS production, both by inhibiting ROS-generating enzymes and by slowing entry of electrons into the electron transport chain. Such a view has recently been hypothesized to explain the significance of widespread S-glutathionylation of mitochondrial proteins in response to oxidative stress [44]. Decreased rates of electron transport may be especially important following inhibition of ATP synthase activity in order to avoid hyperpolarization of the inner mitochondrial membrane and *increased* ROS formation [45].

Oxidant stress in the cytosol should lead to inhibition of the activity of GAPDH and possibly other glycolytic enzymes, promoting a rerouting of glucose metabolism to the PPP to generate cytosolic NADPH [8]. In fact, our findings reveal the essential catalytic thiol of Cys150 and a nearby thiol at Cys154 (Supplementary Table S1) to be likely participants in an inhibitory disulfide bond in GAPDH. Adoption, by GAPDH, of the conformation required to form this disulfide may require prior S-glutathionylation [46]. In addition, we have reported previously that the glycolytic enzyme triosephosphate isomerase, also identified here, becomes very highly enriched among proteins containing reversibly oxidized thiols in homogenates from rat brains not frozen quickly after euthanasia [20], a change that is linked to a profound increase in protein S-glutathionylation in these brains [22].

The postulated global shift in metabolism from ATP supply to antioxidant support in response to oxidative stress would require that major ATP-consuming processes be at least partially inhibited to prevent a precipitous fall in ATP levels during restoration of redox homeostasis. In neurons, these processes include Na^+, K^+-ATPase activity

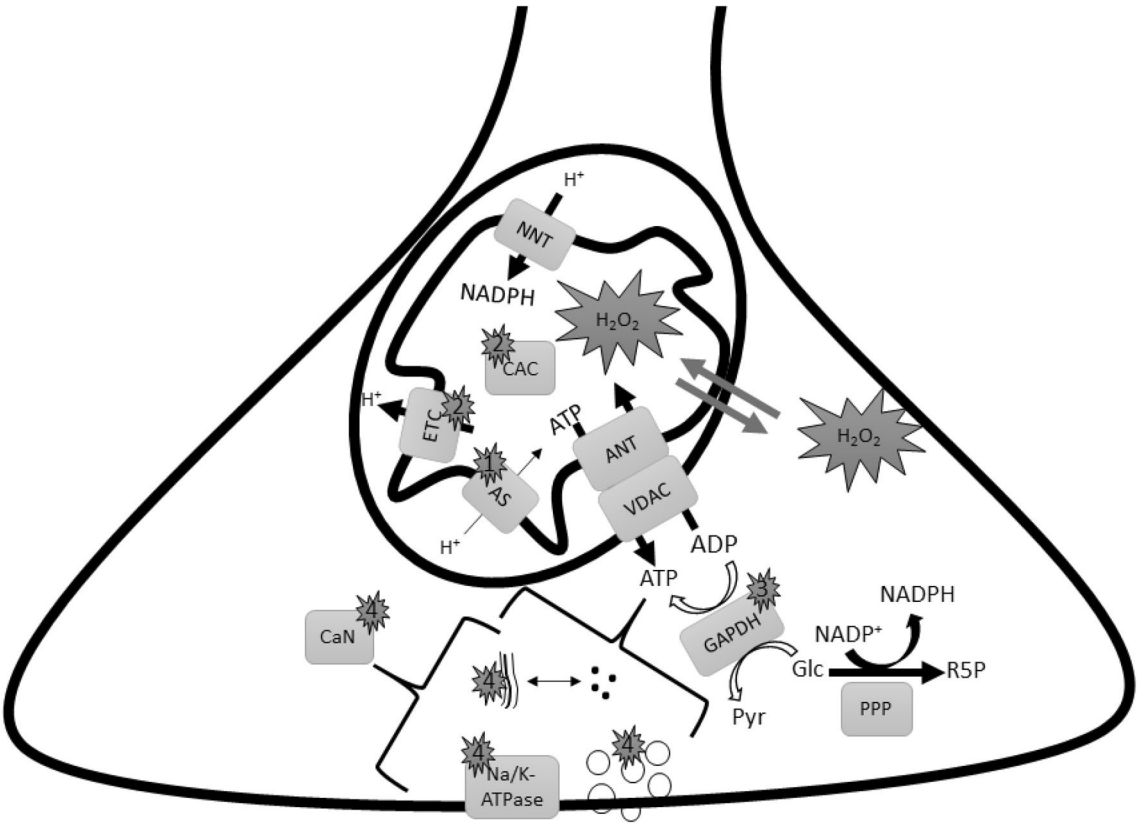

Fig. 4 Proposed roles of reversible oxidations of protein thiols in the adaptation of synaptic compartments to oxidant stress. (1) Oxidative inhibition of ATP synthase (AS) activity should make more energy available from the inner mitochondrial H^+ gradient to drive NADPH production by the nicotinamide nucleotide transhydrogenase (NNT). (2) Oxidative inhibition of the citric acid cycle (CAC) and electron transport complexes (ETC) should decrease mitochondrial ROS generation both by impairing specific sites of ROS generation and by slowing entry of electrons into the electron transport chain. (3) Inhibition of the activity of GAPDH and other glycolytic enzymes should divert glucose metabolism to the pentose phosphate pathway (PPP) to generate NADPH necessary to combat cytosolic oxidant stress. (4) Rerouting metabolism away from ATP synthesis and towards oxidant protection would require coordinated oxidative inhibition of major ATP-consuming processes, including Na^+, K^+-ATPase activity and the recycling of both synaptic vesicles and actin filaments, to prevent a deleterious fall in ATP levels. Oxidative inhibition of the phosphatase activity of CaN should further inhibit these processes, at least in presynaptic terminals, by facilitating stable protein phosphorylation by protein kinases

[47], synaptic vesicle cycling [48], and actin dynamics [47]. Synaptosomal proteins mediating all of these activities were found here to be targeted by thiol oxidations. Furthermore, oxidations to a presumed disulfide bond of the PAO-binding thiols of CaN, shown here for the first time to occur in presynaptic compartments, in vivo, may also be significant is this regard. Oxidation of the PAO-binding vicinal thiols of CaN by hydrogen peroxide, added in vitro, were previously found to inhibit the catalytic activity of the enzyme [49]. Inhibition of CaN activity would be expected to inhibit (i) Na^+, K^+-ATPase activity [28], (ii) synaptic endocytosis [29], and dissociation of actin filaments [50], all by promoting protein phosphorylation. Lastly, we suggest that oxidative inhibition of these activities may contribute to the well-established inhibition of synaptic transmission by hydrogen peroxide [1].

The biotin-switch/avidin-affinity method, which was investigated here as a complementary approach to assessing the reversibly oxidized thiol proteome of synaptosomes, produced an apparent fivefold lower yield of oxidized proteins than did the redox PAO-affinity method. The greater yield of oxidized proteins obtained by the redox PAO-affinity method may relate, at least in part, to not having to remove TCEP prior to the capture, by PAO binding, of proteins containing formerly oxidized thiols (Fig. 1). In the biotin-switch method, removal of TCEP prior to addition of the biotin-HPDP may have permitted re-oxidation of oxidant-prone protein thiols. In addition, labeling of protein thiols with biotin-HPDP may be reversed following attack of the resulting mixed disulfide by a second, proximal, protein thiol. Therefore, proteins containing sequentially or conformationally vicinal thiols may not be labeled effectively by the

biotin-switch technique. This may explain why some of the most abundant proteins in the oxidized protein fraction from the PAO-affinity method, for example the 75 kDa subunit of complex I, were not also identified by the biotin-switch procedure. Indeed, two of the reversibly oxidized cysteine residues identified on this protein, namely C176 and C179, are sequentially vicinal (Supplementary Table S1). On the other hand, the biotin-switch method should be better able to label proteins that undergo oxidations at thiols that are regionally-isolated and not part of a thiol pair capable of binding to PAO. Despite the lower yield of oxidized proteins captured by the biotin-switch approach, and the probable inability of this method to tag some oxidized proteins, the results of the biotin-switch experiments further established the alpha subunit of the mitochondrial ATP synthase as a selective target of reversible thiol oxidations in synaptosomes.

In summary, the results of this study establish the reducible disulfide proteome of synaptosomes under conditions designed to limit postmortem thiol oxidations and identify the alpha subunit of mitochondrial ATP synthase as a preferential target of thiol oxidative pathways operating in the brain. We propose that the reversible oxidations of thiols on the synaptosomal proteins identified here may facilitate a rapid metabolic reprogramming in neurons necessary to support termination of hydrogen peroxide signaling and to protect against oxidative stress. Chronic oxidant-induced rewiring of synaptic metabolism, however, may contribute to impairment of synaptic transmission and viability in neurodegenerative disorders [4]. Elucidation of the specific pathways underlying oxidations of protein thiols in synaptosomes and a complete understanding of the physiological and pathological significance of these oxidations awaits further investigations.

Acknowledgements The authors thank the University of Scranton for the financial support for this work. They also thank Ms. Courtney Higgins for technical support and Mr. Richard Trygar for administrative support and of this project.

Author Contributions TDF designed the study, supervised the performance of the work and the collection and analyses of data, and wrote most of the manuscript. GM and MCA performed all of the laboratory work, including refinement of methods, and contributed to data analyses and manuscript preparation. All authors approved the final paper.

Funding This work was not supported by external funding.

Compliance with Ethical Standards

Conflict of interest The authors declared that they have no conflict of interest.

Ethical Approval The study was approved by the Institutional Animal Care and Use Committee of the University of Scranton (2019, Protocol #7-19).

References

1. Massaad CA, Klann E (2011) Reactive oxygen species in the regulation of synaptic plasticity and memory. Antioxid Redox Signal 14:2013–2054. https://doi.org/10.1089/ars.2010.3208
2. Hongpaisan J, Winters CA, Andrews SB (2004) Strong calcium entry activates mitochondrial generation, upregulating kinase signaling in hippocampal neurons. J Neurosci 24:10878–10887. https://doi.org/10.1523/JNEUOSCI.3278-04.2004
3. Cobley JN (2018) Synapse pruning: Mitochondrial ROS with their hands on the shears. BioEssays 40:e1800031. https://doi.org/10.1002/bies.201800031
4. Foley TD (2019) Reductive reprogramming: A not-so-radical hypothesis of neuro-degeneration linking redox perturbations to neuroinflammation and excitotoxicity. Cell Mol Neurobiol 39:577–590. https://doi.org/10.1007/s10571-019-00672-w
5. Papadia S, Soriano FX, Leveille F, Martel MA, Dakin KA, Hansen HH, Kaindl A, Sifringer M, Fowler J, Stefovska V, McKenzie G, Craigon M, Corriveau R, Ghazal P, Horsburgh K, Yankner BA, Wyllie DJ, Ikinomidou C, Hardingham GE (2008) Synaptic NMDA receptor activity boosts intrinsic antioxidant defenses. Nat Neurosci 11:476–487. https://doi.org/10.1038/nn2071
6. Baxter PS, Bell KF, Hasel P, Kaindl AM, Fricker M, Thomson D, Cregan SP, Gillingwater TH, Hardingham GE (2015) Synaptic NMDA receptor activity is coupled to the transcriptional control of the glutathione system. Nat Commun 6:6761. https://doi.org/10.1038/ncomms7761
7. Ren X, Zou L, Zhang X, Branco V, Wang J, Carvalho C, Holmgren A, Lu J (2017) Redox signaling mediated by thioredoxin and glutathione systems in the central nervous system 27:989–1010. https://doi.org/10.1089/ars.2016.6925
8. Rasler M, Wamelink MM, Kowald A, Gerisch B, Heeren G, Struys EA, Klipp E, Jakobs C, Breitenbach M, Lehrach H, Krobitsch S (2007) Dynamic rerouting of the carbohydrate flux is key to counteracting oxidative stress. J Biol 6:10. https://doi.org/10.1186/jbiol61
9. Peralta D, Bronowska AK, Morgan B, Doka E, Van Laer K, Grater F, Dick TP (2015) A proton relay enhances H_2O_2 sensitivity of GAPDH to facilitate metabolic adaptation. Nat Chem Biol 11:156–163. https://doi.org/10.1038/nchembio.1720
10. Lu J, Holmgren A (2014) The thioredoxin antioxidant system. Free Radic Biol Med 66:75–87. https://doi.org/10.1016/j.freeradbiomed.2013.07.036
11. Randall LM, Ferrer-Sueta G, Denicola A (2013) Peroxiredoxins as preferential targets in H_2O_2-induced signaling. Methods Enzymol. 527:41–63. https://doi.org/10.1016/B978-0-12-405882-8.00003-9
12. Chiu J, Hogg PJ (2019) Allosteric disulfides: sophisticated molecular structures enabling flexible protein regulation. J Biol Chem 294:2929–2960. https://doi.org/10.1074/jbc.REV118.005604
13. Saurin AT, Neubert H, Brennan JP, Eaton P (2004) Widespread sulfenic acid formation in tissues in response to hydrogen peroxide. Proc Natl Acad Sci USA 101:17982–17987. https://doi.org/10.1073/pnas.0404762101
14. Eaton P, Shattock MJ (2002) Purification of proteins susceptible to oxidation at cysteine residues: identification of malate dehydrogenase as a target for S-glutathionylation. Ann NY Acad Sci 973:529–532. https://doi.org/10.1111/j.1749-6632.2002.tb04694.x
15. Lind C, Gerdes R, Hammell Y, Schuppe-Koistinen I, von Lowenhielm HB, Holmgren A, Cotgreave IA (2002) Identification of S-glutathionylated cellular proteins during oxidative stress and constitutive metabolism by affinity purification and proteomic analysis. Arch Biochem Biophys 406:229–240. https://doi.org/10.1016/s0003-9861(02)00468-x

16. Rehder DS, Borges CR (2010) Cysteine sulfenic acid as an intermediate in disulfide bond formation and nonenzymatic protein folding. Biochemistry 49:7748–7755. https://doi.org/10.1021/bi1008694
17. Beer SM, Taylor ER, Brown SE, Dahm CC, Costa NJ, Runswick MJ, Murphy MP (2004) Glutaredoxin 2 catalyzes the reversible oxidation and glutathionylation of mitochondrial membrane thiols proteins: Implications for mitochondrial redox regulation and antioxidant DEFENSE. J Biol Chem 279:47939–47951. https://doi.org/10.1074/jbc.M408011200
18. Wolhuter K, Whitwell HJ, Switzer CH, Burgoyne JR, Timms JF, Eaton P (2018) Evidence against stable protein S-nitrosylation as a widespread mechanism of post-translational regulation. Mol Cell 69:438–450. https://doi.org/10.1016/j.molcel.2017.12.019
19. Stocker S, Van Laer K, Mijuskovic A, Dick TP (2018) The conundrum of hydrogen peroxide signaling and the emerging role of peroxiredoxins as redox relay hubs. Antioxid Redox Signal 28:558–573. https://doi.org/10.1089/ars.2017.7162
20. Foley TD, Stredny CN, Coppa TM, Gubbiotti MA (2010) An improved phenylarsine oxide-affinity method identifies triose phosphate isomerase as a candidate redox receptor protein. Neurochem Res 35:306–314. https://doi.org/10.1007/s11064-009-0056-z
21. Adams E, Jeter D, Cordes AW, Kolis JW (1990) Chemistry of organometalloid complexes with potential antidotes: structure of an organoarsenic(III) dithiolate ring. Inorg Chem 248:1500–1503
22. Foley TD, Cantarella KM, Gillespie PF, Stredny ES (2014) Protein vicinal thiol oxidations in the healthy brain: not so radical links between physiological oxidative stress and neural cell activities. Neurochem Res 39:2030–2039. https://doi.org/10.1007/s11064-014-1378-z
23. Li R, Kast J (2017) Biotin switch assays for quantitation of reversible cysteine oxidation. Methods Enzymol 585:269–284. https://doi.org/10.1016/bs.mie.2016.10.006
24. Michaelis ML, Jiang L, Michaelis EK (2017) Isolation of synaptosomes, synaptic plasma membranes, and synaptic junctional complexes. Methods Mol Biol 1538:107–119. https://doi.org/10.1007/978-1-4939-6688-2_9
25. Mi H, Muruganujan A, Casagrande JT, Thomas PD (2013) Large-scale gene function analysis with the PANTHER classification system. Nat Protocol 8:1551–1566. https://doi.org/10.1038/nprot.2013.092
26. Lundgren DH, Hwang SI, Wu L, Han DK (2010) Role of spectral counting in quantitative proteomics. Expert Rev Proteomics 7:39–53. https://doi.org/10.1586/epr.09.69
27. Thomas GD, O'Rourke B, Sikkink R, Marban E, Victor RG (1997) Differential modulation of cortical synaptic activity by calcineurin (phosphatase 2B) versus phosphatases 1 and 2A. Brain Res 749:101–108. https://doi.org/10.1016/s0006-8993(96)01305-4
28. Marcaida G, Kosenko E, Minana MD, Grisolia S, Felipo V (1996) Glutmate induces a calcineurin-mediated dephosphorylation of Na+, K(+)-ATPase that results in its activation in cerebellar neurons in culture. J Neurochem 66:99–104. https://doi.org/10.1046/j.1471-4159.1996.66010099.x
29. Sun T, Wu XS, Xu J, McNeil BD, Pang ZP, Yang W, Bai L, Qadri S, Molkentin JD, Yue DT, Wu LG (2010) The role of calcium/calmodulin-activated calcineurin in rapid and slow endocytosis at central synapses. J Neurosci 30:11838–11847. https://doi.org/10.1523/JNEUROSCI.1481-10.2010
30. Foley TD, Katchur KM, Gillespie PF (2016) Disulfide stress targets modulators of excitotoxicity in otherwise healthy brains. Neurochem Res 41:2763–2770. https://doi.org/10.1007/s11064-016-1991-0
31. Gevondyan NM, Gevondyan VS, Modyanov NN (1993) Location of disulfide bonds in the Na+, K(+)-ATPase alpha subunit. Biochem Mol Biol Int 30:347–355
32. Bencsath FA, Shartava A, Monteiro CA, Goodman SR (1996) Identification of the disulfide-linked peptide in irreversibly sickled cell beta-actin. Biochemistry 35:4403–4408. https://doi.org/10.1021/bi960063n
33. Chaudhuri AR, Khan IA, Luduena RF (2001) Detection of disulfide bonds in bovine brain tubulin and their role in protein folding and microtubule assembly in vitro: a novel disulfide detection approach. Biochemistry 40:8834–8841. https://doi.org/10.1021/bi0101603
34. Halestrap AP, Woodfield KY, Connern CP (1997) Oxidative stress, thiol reagents, and membrane potential modulate the mitochondrial permeability transition by affecting nucleotide binding to the adenine nucleotide translocase. J Biol Chem 272:3346–3354. https://doi.org/10.1074/jbc.272.6.3346
35. Uniprot Consortium (2019) Uniprot: A worldwide hub of protein knowledge. Nucleic Acids Res 47:D506–D515. https://doi.org/10.1093/nar/gky1049
36. Garcia J, Han D, Sancheti H, Yap LP, Kaplowitz N, Cadenas E (2010) Regulation of mitochondrial glutathione redox status and protein glutathionylation by respiratory substrates. J Biol Chem 285:39646–39654. https://doi.org/10.1074/jbc.M110.164160
37. Cobley JN, Noble A, Jimenez-Fernandez E, Valdivia Moya MT, Guille M, Husi H (2019) Catalyst-free click PEGylation reveals substantial mitochondrial ATP synthase subunit alpha oxidation before and after fertilisation. Redox Biol 26:101258. https://doi.org/10.1016/j.redox.2019.101258
38. Cobley J, Nobe A, Bessell R, Guille M, Husi H (2020) Reversible thiol oxidation inhibits the mitochondrial ATP synthase in *Xenopus laevis* oocytes. Antioxidants 9:E215. https://doi.org/10.3390/antiox9030215
39. Bianchet MA, Hullihen J, Pedersen PL, Amzel LM (1998) The 2.8-A structure of rat liver F1-ATPase: configuration of a critical intermediate in ATP synthesis/hydrolysis. Proc Natl Acad Sci USA 95:11065–11070. https://doi.org/10.1073/pnas.95.19.11065
40. Wouters MA, Fan SW, Haworth NL (2010) Disulfides as redox switches: from molecular mechanisms to functional significance. Antioxid Redox Signal 12:53–91. https://doi.org/10.1089/ARS.2009.2510
41. Petrushanko IY, Yakushev S, Mitkevich VA, Kamanina YV, Ziganshin RH, Meng X, Anashkina AA, Makro A, Lopina OD, Gasmann M, Makarov AA, Bogdanova A (2012) S-Glutathionylation of the Na, K-ATPase catalytic α subunit is a determinant of the enzyme redox sensitivity. J Biol Chem 287:32195–32205. https://doi.org/10.1074/jbc.M112.391094
42. Drechsel DA, Patel M (2010) Respiration-dependent H2O2 removal in brain mitochondria via the thioredoxin/peroxiredoxin system. J Biol Chem 285:27850–27858. https://doi.org/10.1074/jbc.M110.101196
43. Mailloux RJ (2018) Mitochondrial antioxidants and the maintenance of cellular hydrogen peroxide levels. Oxid Med Cell Longevity 2018:7857251. https://doi.org/10.1155/2018/7857251
44. Mailloux RJ (2020) Protein S-glutathionylation reactions as a global inhibitor of cell metabolism for the desensitization of hydrogen peroxide signals. Redox Biol 32:101472. https://doi.org/10.1016/j.redox.2020.101472
45. Martinez-Reyes I, Cuezva JM (2014) The H(+)-ATPase: a gate to ROS-mediated cell death or cell survival. Biochim Biophys Acta 1837:1099–1112. https://doi.org/10.1016/j.bbabio.2014.03.010
46. Barinova KV, Serebryakova MV, Muronetz VI, Schmalhausen EV (2017) S-Glutathionylation of glyceraldehyde-3-phosphate dehydrogenase induces formation of C150–C154 intrasubunit disulfide bond in the active site of the enzyme. Biochim Biophys Acta 1861:3167–3177. https://doi.org/10.1016/j.bbagen.2017.09.008

47. Bernstein BW, Bamburg JR (2003) Actin-ATP hydrolysis is a major energy drain for neurons. J Neurosci 23:1–6
48. Rangaruju V, Calloway N, Ryan TA (2014) Activity-driven local ATP synthesis is required for synaptic function. Cell 156:825–835. https://doi.org/10.1016/j.cell.2013.12.042
49. Bogumil R, Namgaladze D, Schaarschmidt D, Schmactel T, Hellstern S, Mutzel R, Ullrich V (2000) Inactivation of calcineurin by hydrogen peroxide and phenylarsine oxide. Evidence for a dithiol-disulfide equilibrium and implications for redox regulation. Eur J Biochem 267:1407–1415. https://doi.org/10.1046/j.1432-1327.2000.01133.x
50. Halpain S, Hipolito A, Saffer L (1998) Regulation of F-actin stability in dendritic spines by glutamate receptors and calcineurin. J Neurosci 18:9835–9844